NJC

Accepted Manuscript

This article can be cited before page numbers have been issued, to do this please use: U. N. Guria, K. Maiti, S. S. Ali, S. K. Samanta, D. Mandal, R. Sarkar, P. Datta, A. K. Ghosh and A. K. Mahapatra, *New J. Chem.*, 2018, DOI: 10.1039/C7NJ04632D.

This is an Accepted Manuscript, which has been through the Royal Society of Chemistry peer review process and has been accepted for publication.

Accepted Manuscripts are published online shortly after acceptance, before technical editing, formatting and proof reading. Using this free service, authors can make their results available to the community, in citable form, before we publish the edited article. We will replace this Accepted Manuscript with the edited and formatted Advance Article as soon as it is available.

You can find more information about Accepted Manuscripts in the author guidelines.

Please note that technical editing may introduce minor changes to the text and/or graphics, which may alter content. The journal's standard Terms & Conditions and the ethical guidelines, outlined in our author and reviewer resource centre, still apply. In no event shall the Royal Society of Chemistry be held responsible for any errors or omissions in this Accepted Manuscript or any consequences arising from the use of any information it contains.

ROYAL SOCIETY OF CHEMISTRY

View Article Online
DOI: 10.1039/C7NJ04632D
Dynamic Article Links ►

Cite this: DOI: 10.1039/c0xx00000x

www.rsc.org/xxxxxx

ARTICLE TYPE

Reaction-Based Bi-signaling Chemodosimeter Probe for Selective Detection of Hydrogen Sulfide and Cellular Studies

Uday Narayan Guria, [a] Kalipada Maiti,[a] Syed Samim Ali, [a] Sandip Kumar Samanta, [a] Debasish Mandal, [b] Ripon Sarkar, [c] Pallab Datta, [c] Asim Kumar Ghosh,[d] Ajit Kumar Mahapatra*[a]

Received (in XXX, XXX) Xth XXXXXXXXX 20XX, Accepted Xth XXXXXXXXX 20XX
DOI: 10.1039/b000000x

A new quinoline-indolium-based chemical probe (**DPQI)** was synthesized and characterized for selective detection of hydrogen sulphide (H_2S). Probe **DPQI** displays highly selective and sensitive detection of hydrogen sulphide over other allied anions and thiol-containing amino acids in aqueous-DMSO at physiological pH. The probe **DPQI** acting as bi-signaling fluorescent chemodosimeter for selective detection of hydrogen sulphide when excited at different wave lengths. The selectivity was guaranteed by use of the unique nucleophilicity of HS^- for nucleophilic addition to the most electrophilic positively charged centre followed by thiolysis of the dinitrophenyl ether to yield the DNB-SH and fluorescent phenoxide moiety, which led to fluorescence emission 'turn on' and characteristic visual fluorescent color change behavior of the sensing system. This is why the probe **DPQI** showed different optical properties at varying concentration of hydrogen sulphide. The structural and electronic properties of the probe (**DPQI**) and its thiolysis product have been demonstrated using ab initio density functional theory (DFT) combined with time-dependent density functional theory (TDDFT) calculations. Utilizing this probe, we have successfully detected hydrogen sulphide in live cells.

Introduction

Hydrogen sulfide (H_2S) is well-known as a volatile toxic gas with the characteristic foul-smell of rotten eggs. Now, it is also considered the third most important gasotransmitter for regulating cardiovascular, neuronal, immune, endocrine, and gastrointestinal systems, along with nitric oxide and carbon monoxide.[1]H_2S contributes to a broad array of physiological responses to maintain cellular health, including vasodilation,[2] angiogenesis, [3] oxygen sensing,[4] apoptosis,[5] inflammation,[6] and neuromodulation, [7] and it can also protect against ischemia/reperfusion injury.[8] On the other hand, studies have established that unregulated, abnormal levels of H_2S may contribute to diseases ranging from Alzheimer's disease[9] and Down's syndrome[10] to diabetes[11]and liver cirrhosis.[12] Considering the challenges of measuring this volatile, reactive small molecule to both healthy and disease states is the shortage of methods for selective tracking of H_2S molecule within living biological specimens and biological samples. Therefore, easy and convenient methods have been required for rapid assessment of this biologically and environmentally important species. To date, a large number of sensitive protocols have been reported for sulfide detection. These methods include classical titrimetry[13] electrochemical techniques[14] spectrophotometry[15] chemiluminescence[16] chromatography[17] and fluorimetry[18] .Among these methods, fluorescent detection methods offered a promising opportunity due to the unique advantages of rapidity, sensitivity, convenience, simplicity, easy operation, and low cost. Recently, the ever-expanding toolbox of reaction-based probes employ three primary strategies for H_2S detection, these probes were primarily designed based on: (a) reduction reactions of azide and nitro[19]; (b) nuclephilic reactions[20]; (c) reactions with metal centered coordination complexes such as copper sulfide precipitation.[21] As the pKa of H_2S is 6.8 and it is calculated that 72% of the total H_2S exists as HS^- under physiological conditions.[22]Therefore, H_2S is a strong nucleophile in biological systems that should participate well in nucleophilic reactions. Based on this property, the design of fluorescent probes for H_2S is mainly based on specific chemical reactions by taking advantage of the reducing or nucleophilic properties of H_2S. For example, Lippert-Chang[23] and Wang[24] et al. pioneered an approach of using the reduction of aryl azide with H_2S to amine to sense H_2S, which has been expanded to design azide-containing fluorescent probes by altering fluorophores.[25-30] He et al. used the nucleophilic attack of H_2S on the aldehyde functionality to design a fluorescent probe to sense H_2S.[31] Lin et al. reported a near-infrared fluorescent probe for H_2S based on thiolysis of dinitrophenyl ether.[32]

View Article Online
DOI: 10.1039/C7NJ04632D

Furthermore, a couple of elegant probes have been designed by splitting the dinitrophenyl ether or dinitrobenzenesulfonyl group to restore their original fluorescence.[33] The sulfide anion is a very effective nucleophile and reacts readily with sulfonate esters and thiolysis of aryl nitrate. Not only, being a good nucleophile, it has a tendency to attack positively charged electrophilic centre. This fact provided us with a clue for the design of novel fluorescent probes for the sulfide anion having both the reacting centre in one chromophore. In most of the reported literatures the chemosensors are composed of either ether group linked with the fluorophore moiety or positively charged electrophilic centre. Even in few cases both the reactive centre are present simultaneously. But in those cases only thiolysis of ether occurred and hence fluorescence were regenerated.[34] Furtheremore, Lin et al. reported a typical chemosensor which contain both the reactive centre and both of them react with H_2S to show different optical properties. [35] But, in that particular case the chromophore detecting Cys/GSH/Hcy and H_2S simultaneously. But, there is no report where the probe, composed of dual reacting centre and acting as a dual signaling operator for selective detection of H_2S over the similar reactive biothiols.

Keeping the above in perspective, herein, we have described a dual-reactive groups with dual-functioning colorimetric and fluorometric probe for H_2S with easy structural manipulation by protecting the hydroxyl group with 2,4-dinitrofluorobenzene (DNFB). Here, fluorophore is attached to two reactive groups, DNFB and a highly activated iminium ion acceptor. We named our probe **DPQI** (2-{2-[8-(2,4-Dinitro-phenoxy)-quinolin-2-yl]-vinyl}-1,3,3-trimethyl-3H-indolium) and its quinoline skeleton is used as a color reporting group and the DNB moiety can quench the fluorescence via the photoinduced electron transfer (PET) effect.[36] Thus, the sensor has a very weak initial fluorescence due to intramolecular charge transfer (ICT). Importantly, the probe acting as a dual signaling moiety when excited at different wave length and those signals are arises in different concentration of H_2S. So the novelty of the probe is that two reactive centre shows their reactivity in different concentration of H_2S and exhibits different optical properties. This will finally lead to the enhancement of the good selectivity and high sensitivity of the probe.

Results and discussions

The probe molecule, **DPQI**, was synthesized in three steps (Scheme 1). The reaction of 2-methyl-8-hydroxyquinoline (1) with SeO_2/dioxane results in the formation of aldehyde derivative, **2**, and its hydroxyl group protected by F-DNB under basic conditions yielded the corresponding protected derivative **3**, which, upon coupling with 1,2,3,3-tetramethyl-3H-indolium iodide resulted in **DPQI**. All of the compounds exhibited satisfactory analytical and spectral data as given in the Experimental Section (Fig. S1-S6 †).

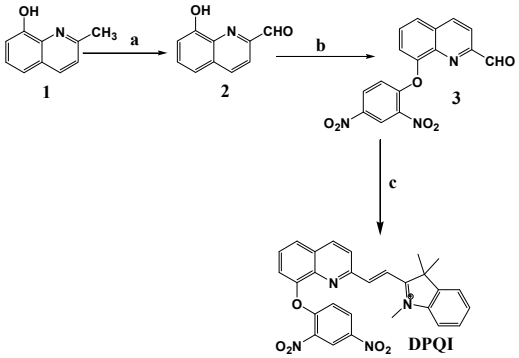

Scheme 1. Synthesis of Probe **DPQI**: Reagents & Conditions: (a) SeO_2, Dioxane, reflux, 12h. (b) 2,4-dinitrofluorobenzene, Et_3N, Dry AcCN, (c) 1,2,3,3-Tetramethyl-3H-indolium iodide, ethanol, rt, 6h.

Colorimetric and Fluorometric response towards H_2S

At first, we tested the spectroscopic properties of **DPQI** (10 μM) by carrying out the fluorescence and absorption titrations of **DPQI** with Na_2S (standard source of H_2S) in aqueous buffer solution (20 mM HEPES buffer, pH 7.4) at 35 °C. The absorption spectra of **DPQI** in presence of H_2S shows some typical character. **DPQI** in aqueous DMSO (1.0 μM, 2:1 v/v) HEPES buffer (pH 7.4) displayed a maximum absorbance at 398 nm and 520 nm responsible for DNB and rest of **DPQI** molecule respectively.

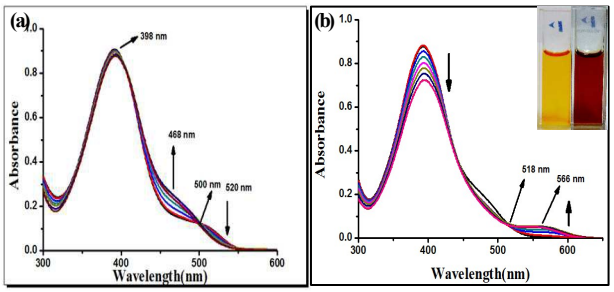

Fig.1. (a) Absorption spectra of **DPQI** (1.0 μM, 20 mM HEPES buffer PH 7.4, DMSO-H_2O; 1:2; v/v) upon gradual addition of Na_2S (0–0.02 mM). (b) Absorption spectra of DPQI (1.0 μM, 20 mM HEPES buffer PH 7.4, DMSO-H_2O; 1:2; v/v) upon gradual addition of Na_2S (0.02-0.1 mM); Inset: color change of DMSO solution of **DPQI** before and after addition of Na_2S.

With increasing concentration of H_2S (0-2 mM), we found that a new peak arises at 468 nm up to 0-0.2 mM concentration of H_2S (20 equiv.) (Fig. 1a). From Fig. 1a it is observed that upon successive addition of H_2S, absorbance intensity at 520 nm is gradually decreased which is accompanied with a strong isosbestic point at 500 nm indicated the formation of new compound. Now, from the Fig. 1a we have noticed a hypsochromic shift occurred in absorbance spectra, which may attribute to the nucleophilic addtion of H_2S to the Indolium moiety thereby blocking the ICT process occurring from quinoline to indolium moiety. Another vision from the graph is that the peak at 398 nm remain undisturbed. This indicates that

View Article Online
DOI: 10.1039/C7NJ04632D

DNB part of the molecule is not cleaved. Thus, formation of isosbestic point and hence formation of new compound and hypsochromic shift in absorbance spectra leads to the formation of **DPQI-SH** adduct at the low concentration of H_2S.

Then, upon increasing the concentration of H_2S up to 0.1 mM (100 equiv) we noticed that the peak intensity at 398 nm gradually decreased and a new peak arises at 566 nm. An isosbestic point was found at 518 nm (Fig. 1b). This result suggested that at high concentration of H_2S, H_2S-mediated cleavage of the electron-withdrawing DNB group releases an oxygen donor at pH 7.4, that increases the push-pull character of the probe and resulting in large bathochromic shifts (at 566 nm) in absorption. So, the bathochromic shift is mainly due to strong Intramolecular Charge Transfer (ICT) within quinolinol moiety. The stoichiometry of the reaction between the probe **DPQI** and Na_2S has been derived to be 1:2 on the basis of a Jobs plot (Fig. S11 †). The pattern of the Jobs plot (both by absorbance and fluorescence method) indicate the stepwise reaction process. Thus the results indicate that H_2S did reaction with dual reaction centers of the probe **DPQI** (Scheme 2). This results also supported by the naked eye color change of the DMSO solution of **DPQI** in presence of H_2S. We have noticed that in addition of small amount of H_2S no significant color change was observed. Whereas when concentration of H_2S was increased color of the solution changed drastically from yellow to deep red (Fig. 1b inset).

In receipt of decent outcome from UV-Vis spectroscopy studies, we went for the fluorescence study. Initially, the probe **DPQI ,** (10 μM in 2:1 water: DMSO mixture at pH 7.4) when excited at 398 nm, exhibit a low intense emission band at 461 nm (Fig. 2a) responsible for weak blue fluorescence [Fig. S12b(i) †].

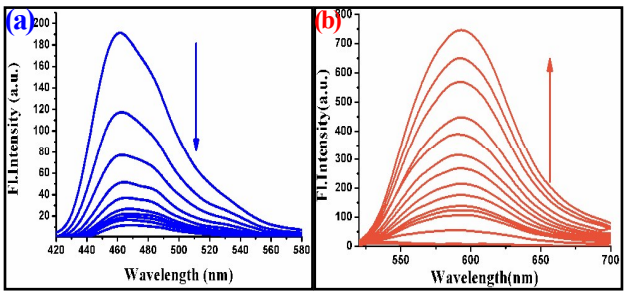

Fig.2. (a) Fluorescence spectra of **DPQI** (λ_{ex} = 398 nm) (1.0 μM, 20 mM HEPES buffer PH 7.4, DMSO-H_2O; 1:2; v/v) upon gradual addition of H_2S (0–0.02 mM). (b) Fluorescence spectra of **DPQI** (λ_{ex} = 500 nm) (1.0 μM, 20 mM HEPES buffer PH 7.4, DMSO-H_2O; 1:2; v/v) upon gradual addition of H_2S (0.02-0.1 mM).

Upon gradual addition of H_2S up to 0.02 mM, this low intense fluorescence band intensity was decreased up to the saturation. It is possible because intramolecular charge transfer (ICT) might occur from the qunoline recognition unit to the indolium moiety, resulting this low intense band, which is consistent with our design strategy that the quinoline fluorescence in **DPQI** is heavily quenched due to PET process occurring between DNB and quinoline moiety.[37] Thus the peak at 461 nm was completely vanished after addition of 20 equiv. of H_2S due to the blocking of ICT process as **DPQI-SH** adduct was formed (Scheme 2). Importantly, we found no other emission band in visible region even addition of higher concentration of H_2S. Then we excited **DPQI** at 500 nm and found no fluorescence band in visible region. Upon incremental addition H_2S (> 20 equiv.) a new emission band at 593 nm was found up to 0.1 mM (Fig. 2b). A deep orange fluorescent color was found in naked eye [Fig. S12b(ii) †]. As the intensity of the newly generated emission reaches the maximum values, we achieved more than 700 fold in increase in fluorescence intensity. These results interpreted that probe **DPQI** attacked by H_2S at a low concentration and produces **DPQI-SH** adduct, while this intermediate product is further attacked by H_2S at a high concentration and thiolysis of ether occurred to yield the orange fluorescent compound **QI-SH** and a non fluorescent DNB-SH. Thus it is clear from above phenomenon that the probe acting as a dual signaling moiety for H_2S. Furthermore, H_2S has decent linear relationships with the maximum intensity values of newly generated emission bands (at 593 nm) in a certain concentration range (Fig. S10 †), and accordingly the limit of detection is calculated to be 3.5 μM.

Selectivity of DPQI towards H_2S

In order to check whether the **DPQI** is sensitive to only H_2S or even to the other anions, similar fluorescence titrations were carried out in the same medium with other different analytes, viz. F^-, Cl^-, Br^-, I^-, SO_4^{2-}, HSO_3^-, AcO^-, CN^-, $H_2PO_4^-$, $S_2O_3^{2-}$ as well as thiol containing amino acids (Cys, Hcy and GSH) and found no significant fluorescence enhancement in the presence of any of these analytes (Fig. S8†). Therefore, **DPQI** is selective to H_2S among other analytes studied. Visual fluorescent color change experiments have been carried out to look at the behavior of **DPQI** in the presence of various anions. Under UV light, the solution of **DPQI** is low intense blue fluorescence whereas in the presence of H_2S, it shows an intense orange fluorescent color which is otherwise not present in case of the other analytes studied (Fig. S13†). Therefore, H_2S can easily be differentiated by visual color change among the other anionic species. In order to show the practical utility of **DPQI** to detect H_2S selectively even in the presence of other analytes, competitive anion titrations were carried out. These studies reveal that the H_2S-induced fluorescence enhancement was unaffected in the presence of allied anions viz; F^-, Cl^-, Br^-, I^-, SO_4^{2-}, HSO_3^-, AcO^-, CN^-, $H_2PO_4^-$, $S_2O_3^{2-}$. In addition, we also performed competitive selectivity studies with some representative thiol containing amino acids (Cys, Hcy and GSH). These experimental results implied that the **DPQI** probe is highly selective toward the H_2S even though the concentration of other competitive analytes is 100 equiv. higher than H_2S concentration (Fig. S9 †). Thus, it is notable that **DPQI** can be used as a selective H_2S fluorescent sensor in the presence of other relevant analytes.

To provide further support for nucleophilic addition followed by the removal of DNB moiety from **DPQI** by H_2S, ESI MS experiment was carried out for analysis of product.

View Article Online
DOI: 10.1039/C7NJ04632D

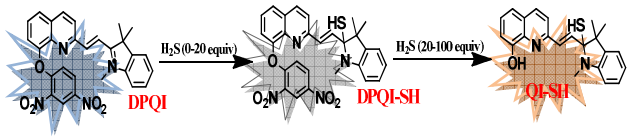

Scheme 2. Mechanism of reaction of H_2S with **DPQI**.

The reaction mechanism of **DPQI** to H_2S could be reasonably explained by a nucleophilic reaction. To know if there happen only nucleophilic addition of H_2S to the indolium moiety or only thiolysis of ether pat or both, we have done mass spectroscopic assay. In ESI-MS analysis the peak at m/z: 528.1517 responsible for **DPQI-SH** adduct. Another peak at m/z: 362.1493 indicating the formation of thiol adduct of quinonilol-indoline i.e. **QI-SH**. Peak at 200.9918 confirm that thiolysis of ether was occurred and **DNB-SH** was formed (Fig. S7 †). Importantly we did not have any peak which might support that only thiolysis of ether was occurred. These results strongly support the two step reaction of the probe with H_2S and most importantly mechanism of the reaction is first thiol addition then thiolysis of ether. To support the stepwise reaction mechanism we have done MS (HRMS) titration also. Upon reaction with 0.5 equiv. of H_2S, we found the peak at m/z: 528.1518 (Fig. S19 †). This peak is the indication of the formation of only **DPQI-SH** adduct. Addition of excess H_2S exhibited a peak at m/z: 362.1496 and at 200.9908 (Fig. S20 †). Nevertheless, the former is for **QI-SH** and latter is responsible for DNB-SH.

Reaction rate investigation

During the experiments, interestingly, we found that the reaction rate between probe **DPQI** and H_2S was affected by the reaction temperature. The reaction is slow at room temperature but quite rapid at 60 ^{0}C (the fluorescence intensity reached saturation within 6 min). However, this temperature was too high to detect H_2S in living cells. On the other hand, the probe exhibited almost the same reaction rate under 35 ^{0}C and 45 ^{0}C conditions (Fig. 3). In both cases the fluorescence intensity took 13 min to reach saturation. Thus, 35 ^{0}C was chosen as the optimal reaction temperature.

Encouraged by these preliminary results, we proceeded to study the reaction kinetics under pseudo-first-order conditions with a large excess of H_2S (>20 equiv.) over probe **DPQI** (10.0 μM) in aqueous DMSO (2:1 v/v) pH 7.4 HEPES buffer at 35 ^{0}C temperature. The pseudo-first-order rate constant k' was calculated as $k' = 0.23$ min^{-1}with the equation[38] $\ln[(F_{max}-F_t)/F_{max}] = -k't$ (Fig. S14a †), where F_t and F_{max} are the fluorescence intensities at 593 nm at time t and the maximum value obtained after the reaction was complete; k' is the observed rate constant. Furthermore, the plots of observe rate constant k' vs. [H_2S] was a straight line passing through the origin, suggesting that the reaction is overall second order with $k_2 = 775.44$ M $^{-1}$s^{-1} (Fig. S15 †). From Fig. 3b, it is obvious that at low concentration of H_2S, nucleophilic reaction towards indolium cation of **DPQI** is much quicker (only 2 min required for saturation). So, the next step reaction i.e. thiolysis of ether through addition elimination of H_2S is the slow step of the reaction and high degree of 2nd order rate constant attribute to proceed the reaction.

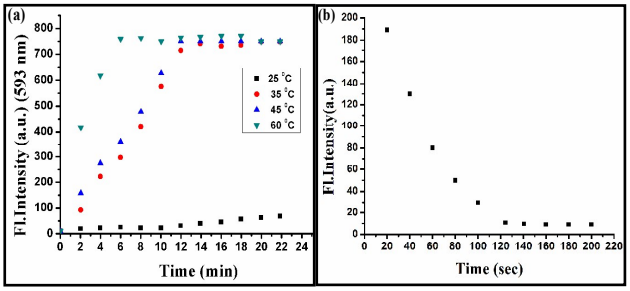

Fig. 3. (a)Time dependent fluorescence change of **DPQI** with H_2S (100 equiv.) as a function of time (at 593 nm). (b) Time dependent fluorescence change of **DPQI** with H_2S (20 equiv) as a function of time (at 461 nm, 35^{0}C).

Density functional theory (DFT) calculations

To get insight into the optical properties of the new probe **DPQI** responding to H_2S, density functional theory (DFT) calculations with the B3LYP exchange functional employing 6-31+G(d,p) basis sets using a suite of Gaussian 09 programs were performed.

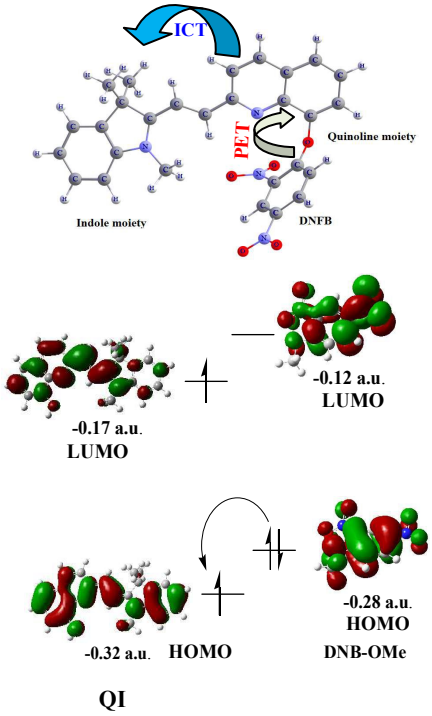

Fig. 4. Top: Energy optimized structure of **DPQI** and its emission response regulated by PET and ICT mechanism. Bottom: FMO energy of DNB-OMe and **QI** at the excited state.

Emission of **DPQI** should be regulated by DNFB *via* photoinduced electron transfer (PET) mechanism. To authenticate the suggested fluorescence mechanism, the frontier orbital energy of both separate **DNB-OME** and **QI** were also calculated. As shown in Fig. 4, the energy of highest occupied molecular orbital (HOMO) of DNB lies between HOMO and lowest unoccupied molecular orbital (LUMO) of **DPQI** molecule.

View Article Online
DOI: 10.1039/C7NJ04632D

This indicate that at excited state electron from HOMO of DNB transfer to the HOMO of the **DPQI** and hence fluorescence is quenched. Consequently, the π-electrons cloud on both the HOMO and LUMO efficiently distribute in the respective quinoline and indole units in **DPQI**, suggesting that **DPQI** is a typical intramolecular charge transfer (ICT)- based fluorophore. These results suggesting the initial low intense blue fluorescence at 461 nm. As, initially **DPQI-SH** adduct was formed the above ICT process was turned off which is responsible for gradual quenching in fluorescence at 461 nm. Whereas, thiolysis of ether part diminish the PET process, producing the phenolate ion, responsible for bathochromic shift both in absorption and emission spectra. Thus, the emission response of **DPQI** to H_2S is delimited by the PET and ICT mechanisms together.

Calculations based on single-excitation time-dependent DFT (TDDFT) were performed to explain the electronic structural properties of the ground and excited states of **DPQI**. The vertical transitions calculated by TDDFT (Table S1 †) were comparable with the experimentally observed UV−vis spectra. The studies suggest that the vertical transitions (HOMO-1→LUMO, f = 0.6002, the highest observed oscillator strength) observed at ~415 nm are comparable to those of the experimentally observed spectra at ~398 nm for **DPQI**. Whereas, HOMO→LUMO (ΔE = 2.96 ev) observed at 495 nm is comparable with the experimental peak at 520 nm. In the case of the phenolate ion, the observed band at ~542 nm is assigned to the transition of HOMO→LUMO (ΔE = 2.58 ev) (Fig. S17 †, Table S2 †) that results from a $\pi \rightarrow \pi^*$ transition and corresponds to the experimental λ_{max} ~566 nm.

Practical application

Intense color change in naked eye as well as in fluorescent in presence and absence of H_2S strongly recommends that the sensors can be used in kits for the detection of H_2S. For the complete study of the practical application of the probe **DPQI**, test strips were made of by dipping TLC plates into acetonitrile solution of **DPQI** (c = 1.0× 10^{-3} M) and then drying them in air. **DPQI** immersed TLC plates were then treated with different concentration of H_2S. As shown in Fig. 5, when concentration of H_2S was increased gradually, a noticeable change in color (from pale yellow to deep brown) of the TLC plates were observed under irradiation at 254 nm under a UV lamp.

Similar phenomenon was also found in case of fluorescence color. When H_2S concentration was increased, the fluorescent color of the test strips changes from weak blue to orange (Fig. 5). Most importantly, during solid state detection of H_2S we observed that high concentration of H_2S was required for the initial color change (both in ambient light and fluorescence). This observation again suggests that two step reactions was occurred. Primarily, some H_2S was consumed for nucleophilic addition to the indolium moiety which has a minute effect to the color and fluorescence properties (pale yellow color and weak blue fluorescence). Secondly, addition of excess H_2S is responsible for thiolysis of dinitrophenyl ether which is accompanied with the color as well as fluorescence change. Therefore, the test strips could conveniently detect H_2S in solutions. The above result suggest that this type of solid system protocol may be used to perform as a sensitive and practical ''dip-in'' naked eye H_2S sensors in the near future.

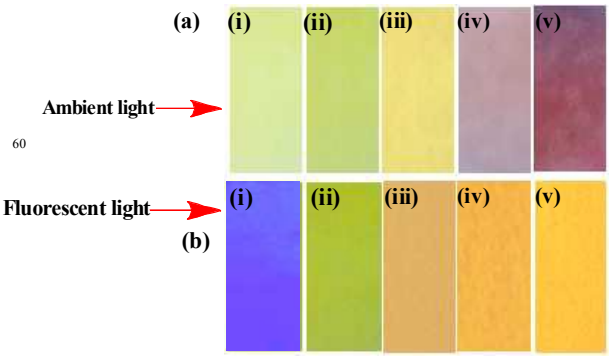

Fig. 5. (a) Naked eye color change of TLC plates (i) **DPQI** (1.0 x 10^{-4} M), (ii) 10.0 x 10^{-4} M Na_2S, (iii) 25.0 x 10^{-4} M Na_2S, (iv) 40.0 x 10^{-4} M Na_2S, (v) 80.0 x 10^{-4} M Na_2S (b) Fluorescent color change (i) **DPQI** (1.0 x 10^{-4} M), (ii) 10.0 x 10^{-4} M Na_2S, (iii) 25.0 x 10^{-4} M Na_2S, (iv) 40.0 x 10^{-4} M Na_2S, (v) 80.0 x 10^{-4} M Na_2S.

Hydrogen sulphide coming as industrial waste materials and mixed with different water resources. Thus, detection of H_2S is very much essential from natural surface water resources where several interfering agents are present. We collected some surface water samples from different areas of West Bengal, India (see Supporting Information for complete details) and experienced the effectiveness of our sensor in detecting H_2S in these various aqueous media.

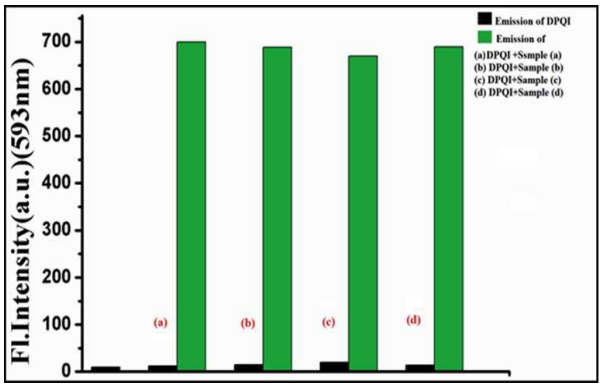

Fig. 6. Sensing of H_2S from surface water sample by using **DPQI**.

To do this, we prepared 10 μM solutions of H_2S in different water samples and observed the change in emission of **DPQI**. In all cases, substantial fluorescence (at 593nm) enhancement were noticed (Fig. 6). These results suggest that irrespective of the source of water, enhancement in fluorescence of **DPQI** is manifested in the presence of H_2S. These results undeniably set up the capability of **DPQI** as a prevalent fluorescent sensor for H_2S.

View Article Online
DOI: 10.1039/C7NJ04632D

Detection of hydrogen sulphide with DPQI in living cells

Next, we evaluate the abilities of **DPQI** to visualize changes in H_2S (here we use Na_2S for standard of H_2S) levels in live-cell imaging mode using fluorescence microscopy (Fig. 7) (detailed of cell study is described in Experimental section). Hence, to know the effectiveness of **DPQI** as a probe for in vitro detection of H_2S by fluorescence microscopy, Vero cells were used to detect endogenous H_2S in live cells. To do this, first we did MTT assay of all the components to see the cell viability (Fig. S18 †). From Fig. S17, it is found that probe **DPQI** hardly has an adverse effect towards the cell; however the H_2S had concentration dependent adverse effect when cells were treated with varying concentrations of H_2S. As shown in the bright field and fluorescence images of the cells incubated only with Na_2S (0.1 mM) for 30 min no fluorescence can be observed (Fig 7a and 7b). After incubating Vero cells with 0.1 μM of **DPQI** for 30 min at 37^0C in presence of Na_2S we found different color inside cells at different concentration of H_2S.

Initially, blue color inside cells was found when the cells were only treated with **DPQI** (Fig. 7d) (blue channel, λ_{ex}=350nm, λ_{em}= 380-480 nm). Then we observed cells in fluorescence microscope with increasing concentration of H_2S. Fluorescence inside cells was tend to vanish when treated with 0.02 mM of H_2S (20 equiv) (Fig. 7e). Upon increasing the concentration (up to 0.1 mM) (red channel λ_{ex}=561 nm, λ_{em}= 585-630 nm) we found that intensity of orange fluorescence inside the cells was gradually increased (Fig. 6f-7h). This result also prove the two step reaction of the probe and H_2S.

The fluorescence microscopic study strongly recommended that probe **DPQI** could readily cross the membrane barrier of the Vero cells, and detect intracellular H_2S.

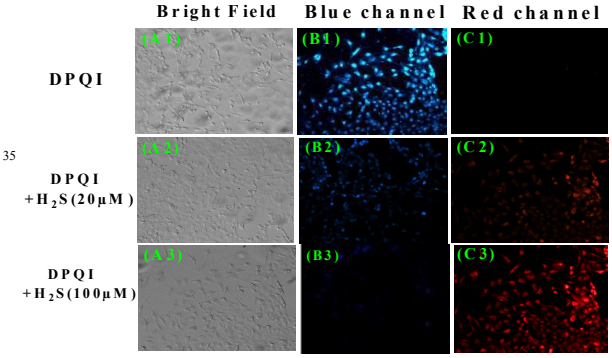

Fig. 7. Fluorescence images of probe in vero cells (40× objective lens): (A1) Bright field image of only cells treated with **DPQI** (0.1 μM) (A2) Bright field image of DPQI treated with 20.0 μM Na_2S (A3) Bright field cell image of DPQI with 100 μM Na_2S. (B1) Blue channel fluorescence images of cells treated with **DPQI** (0.1 μM) (blue channel, λ_{ex}=350nm, λ_{em}= 380-480 nm). (B2) Fluorescence image of **DPQI** (blue channel, λ_{ex}=350nm, λ_{em}= 380-480 nm) treated with 20.0 μM Na_2S. (B3) Fluorescence image of **DPQI** (blue channel, λ_{ex}=350nm, λ_{em}= 380-480 nm) treated with 100 μM Na_2S (C1) Red channel image of cells treated with **DPQI** (0.1 μM) (red channel λ_{ex}=561 nm, λ_{em}= 585-630 nm.). (C2) Red channel Fluorescence image of **DPQI** (red channel λ_{ex}=561 nm, λ_{em}= 585-630 nm.) treated with 20.0 μM Na_2S.. (C3) fluorescence image of **DPQI** inside cells treated with 100 μM Na_2S (red channel λ_{ex}=561 nm, λ_{em}= 585-630 nm.).

It is quite obvious that as bright field images in different cases did not revealed any extensive morphological change the components are cell viable. These findings open up the avenue for future *in vivo* biomedical applications of this probe.

Conclusion

In conclusion, we have synthesized a new quinoline-indolium-based an improved fluorescent probe **DPQI** for H_2S detection. The design was based nucleophilic addition of HS^- to iminium ion followed by thiolysis of dinitrophenyl ether to release the fluorophore. This two-step reaction was observed by slowly increasing concentration of H_2S. Concomitantly, this probe showed fluorescent emission colour changes from colorless to orange and visible colour changes from pale yellow to bright brown at higher concentration in response to H_2S. The probe has a high selectivity for H_2S over competitive analytes. The H_2S sensing mechanism, namely, H_2S triggered addition and then thiolysis reaction, was proved by LC–MS. TDDFT calculations were carried out to demonstrate the electronic properties of **DPQI** and its reaction products. The practical phenomena are fully supported by DFT calculations. Test kit experiment implies that the probe is able to detect H_2S even in solid state. This probe is also applicable to detect H_2S in live cell and has the ability to detect intracellular H_2S.

Experimental Section

Materials and Methods. Unless otherwise mentioned, materials were obtained from commercial suppliers and were used without further purification. ^{1}H and ^{13}C NMR spectra were recorded on a Brucker 400 and 300 MHz instrument. For NMR spectra, DMSO-d_6 and $CDCl_3$ were used as solvent using TMS as an internal standard. Chemical shifts are expressed in δ ppm units and ^{1}H–^{1}H and ^{1}H–C coupling constants in Hz. Mass spectra were carried out using a Waters QTOF Micro YA 263 mass spectrometer. Fluorescence spectra were recorded on a Perkin Elmer Model LS 55 spectrophotometer. UV spectra were recorded on a JASCO V-530 spectrophotometer.

Cell Imaging Study. For fluorescence imaging studies Vero cell (Vero 76, ATCC No CRL-1587) lines, were seeded on sterile 35 mm μ-Dish, glass bottom culture dish (ibidi GmbH, Germany), and incubated at 37 °C in a CO_2 incubator for 24-30 hours. The next day, cells were washed three times with phosphate buffered saline (PBS) and fixed using 4% paraformaldehyde in PBS (pH 7.4) for 10 minutes at room temperature. Thereafter the cells were washed with PBS followed by permeabilization using 0.1% saponin for 10 min followed by incubation with 1.0×10^{-7} M of probe **DPQI** dissolved in 100 μL DMEM at 37 °C for 1 h in a

View Article Online
DOI: 10.1039/C7NJ04632D

CO_2 incubator. Before microscopic imaging, all the solutions were aspirated and mounted on slides in a mounting medium containing DAPI (1 μg/mL) and stored in dark before microscopic images were acquired. The cells were observed under Andor spinning disk confocal microscope (SD-CM) with excitation at 350 nm monochromatic laser beam and the collected range of emission wavelength was between 420 and 480 nm (blue channel) and excited at 561 nm and the collected range of emission wavelength was between 585 and 630 nm (red channel). Cells were imaged live by SD-CM 63× oil-immersion objective. Images were acquired in z-stacks of 28 planes at 0.3-μm intervals with 400-ms exposure times every 20 seconds over a period of 30 minutes. In another dish new cells were again cultured in the same manner followed by treatment with Na_2S (0.1 mM). Thereafter the cells were washed thrice with PBS (pH 7.4) to remove any excess Na_2S and incubated in DMEM containing probe DPQI. Finally the cells were washed again with PBS (pH 7.4) three times to remove excess probe outside the cells. The emissions were obtained at above recommended wave length for different concentration of Na_2S (blue channel for low concentration and red channel for high concentration).

Cytotoxic effect on Cells. The cytotoxic effects of DPQI and Na_2S were determined by MTT assay following the manufacturer's instruction (MTT 2003, Sigma-Aldrich, MO). Vero cells were seeded onto 96-well plates (approximately 104 cells per well) for 24 h. Next day media was removed and various concentrations of probe DPQI, Na_2S (0, 15, 25, 50, 75, and 100 μM) made in DMEM were added to the cells and incubated for 24 h. Solvent control samples (cells treated with DMSO in DMEM), no cells and cells in DMEM without any treatment were also included in the study. Following incubation, the growth media was removed, and fresh DMEM containing MTT solution was added. The plate was incubated for 3−4 h at 37°C. Subsequently, the supernatant was removed, the insoluble colored formazan product was solubilized in DMSO, and its absorbance was measured in a micro titer plate reader (Perkin-Elmer) at 570 nm.

Computational Methods. Geometries have been optimized using the B3LYP/6-31G (d, p) level of theory. The geometries are verified as proper minima by frequency calculations. Time-dependent density functional theory calculation has also been performed at the same level of theory. All calculations have been carried out using Gaussian 09 program.

General method of UV-vis and fluorescence titration. For UV-vis and fluorescence titrations, stock solution of Probe **DPQI** was prepared (c = 10.0 μM) in H_2O–DMSO (2:1, v/v) solution (20.0 mM HEPES buffer, pH 7.4).The solution of the guest analytes in the order of 1.0×10^{-3} ML^{-1} was also prepared in H_2O–DMSO (2:1, v/v) solution (20.0 mM HEPES buffer, pH 7.4). The test solution of sensor Probe 1 was prepared by proper dilution method. The spectra of these solutions were recorded by means of UV-vis and the fluorescence methods. All the solvents were purchased from local suppliers and were distilled by standard procedure before use.

Synthesis and Structure Characterization.

Preparation of 2-Formyl-8-Hydroxy-Quinoline (2): A mixture of Selenium dioxide (1041.92mg, 9.378mmol), (dissolved in a minimum amount of water), and 2-methyl-8-hydroxyquinolinol (**1**) (1500mg, 9.423mmol) were dissolved in 1, 4-dioxane.The resultant reactant mixture was refluxed for 2-3hours. After the completion of the reaction (TLC monitored) the crude product was subjected to filtration, while in hot condition, followed by purification of the filtrate obtained, by the column chromatography on silica gel (Hexane: EtOAc; 8:2(v/v)).A light yellow powder obtained. The yield of the crude product is 1065mg. (65.33%), M.P. =102^0C: **IR: KBr (Cm^{-1}):** 3466, 2815, 1711.MS (HR MS): (m/z, %): 174.0547 [($M+H^+$), 100 %]

***Preparation of O -protected 2-Formyl-8-Hydroxy-Quinoline* (3):** A mixture of compound **2** (150 mg, 0.86 mmol), 2,4-dinitrofluorobenzene(165mg, 0.9mmol) and triethylaminewere dissolved in dry acetonitrile. The reaction mixture was refluxed. After the completion of the reaction (TLC monitored), solvent was evaporated in vacuum. Water was added to the reaction mixture and the organic part of the mixture was separated by using dichloromethane (2×30 ml). The combine organic layer was then purified by column chromatography. A yellow crystalline compound of **3** was obtained as a pure product. The yield of the crude product is 51.2mg (80.15%), MS (HR MS): (m/z, %): 340.0509 [($M+H^+$), 100 %];. ^{1}H-NMR (DMSO-d6, 300 MHz): δ (ppm) 7.06 (d, 1H, J=9.0Hz), 7.88 (m, 2H), 8.01 (d,1H,J= 9.0Hz), 8.10 (m, 1H), 8.26 (m, 1H), 8.70 (d,1H,J=9.0Hz), 8.92 (d,1H, J=3.4Hz), 9.94 (1H,s).

Preparation of DPQI: Ethanolic solution compound **3** (95mg, 0.280mmol) was added with 1,2,3,3-Tetramethyl-3H-indolium iodide (48mg, 0.28mmol) and reflux for overnight, a redcolor precipitate was appeared during stirring at room temperature, washed with EtOH. Then the solid was re-crystallized from EtOH-ether (3:2; v/v) mixture to afford pure **DPQI** as a red soil. Yield: 78 mg (56 %), M.P.> 250ºC. MS (HR MS): (m/z, %): 495.1451 [(M^+), 100 %];.^{1}H-NMR ($CDCl_3$, 400 MHz): δ (ppm)1.24 (s, 6H), 1.81 (s, 3H), 6.92 (d, 2H,J=9.2Hz), 7.61 (t, 4H, J=9.0Hz), 7.75 (t, 2H,J=6.0Hz), 7.88 (d, 1H,J=9.0Hz),8.01 (d, 1H,J=12.0Hz), 8.24(m,1H,J=5.4Hz), 8.93(d,1H,J=6.0Hz), 8.57(d,1H,J=12.0Hz), 8.86(d,1H, J=8.1Hz). ^{13}C-NMR (DMSO-d6, 100 MHz): δ (ppm) 24.96, 35.02, 49.23, 52.62, 56.94, 110.12, 115.73, 122.24, 125,17, 127.37, 128.79, 129.32, 129.78, 130.18, 134.05, 138.82, 142.07, 143.87, 143.92, 147.82, 149.42, 150.85, 152.56, 153.72, 162.53, 166.03, 181.73.

Acknowledgements

We gratefully acknowledge DAE-BRNS [Project No. 36(1)/14/12/2016-BRNS/36012] for financial support. SSA thanks to UGC-MANF (Student ID: 2015-17-WES-67786), New Delhi for the financial and research support.

View Article Online
DOI: 10.1039/C7NJ04632D

Conflicts of interest

There are no conflicts to declare

Author information

[a] Department of Chemistry, Indian Institute of Engineering Science and Technology, Shibpur, Howrah-711103, West Bengal, India, Email: akmahapatra@rediffmail.com, Fax: +913326684564

[b] School of Chemistry and Biochemistry, Thapar Institute of Engineering and Technology, Patiala 147 004 Punjab, 486 India.

[c] Centre for Healthcare Science and Technology, Indian Institute of Engineering Science and Technology, Shibpur, India

[d] Bhabha Atomic Research Centre,Trombay.Mumbai-400085, India.

†Electronic Supplementary Information (ESI) available: [details of any supplementary information available should be included here]. See DOI: 10.1039/b000000x/

Notes and References

1. (a) H. Kimura, *Amino Acids* 2011, **41**, 113. (b) D. R. Linden, *Antioxid. Redox Signaling*, 2014, **20**, 818. (c) S. Fiorucci, E. Distrutti, G. Cirino and J. L. Wallace, *Gastroenterology*, 2006, **131**, 259. (d) C. Szabó, *Nature Reviews Drug Discovery* 2007, **6**, 917. (e) O. Kabil and R. Banerjee, *Journal of Biological Chemistry* 2010, **285**, 21903.

2. G.Yang, L. Wu, B. Jiang, B.Yang, J. Qi, Cao. K, Q. Meng, A.K.Mustafa, W. Mu, S.Zhang, S. H. Snyder and R.Wang, *Science* 2008, **322**, 587–590.

3. A. Papapetropoulos, A. Pyriochou, Z. Altaany, G. Yang, A. Marazioti, Z. Zhou, M. G. Jeschke, L. K. Branski, D. N. Herndon and R.Wang, Szabo, C. *Proc. Natl. Acad. Sci. U.S.A*. 2009, 106, 21972–21977.

4. Y.J. Peng, J. Nanduri, G. Raghuraman, D. Souvannakitti, M. M. Gadalla and G. K. Kumar, *Proc. Natl. Acad. Sci. U.S.A*. 2010, **107**, 10719–10724.

5. G. Yang, L.Wu and R. Wang, *FASEB J*. 2006, **20**, 553–555.

6. L. Li, M. Bhatia, Z. Zhu, Y. Zhu, C. Y. R. D. Ramnath, Z. J. Wang, F. B. Anuar, M. Whiteman, M. Salto-Tellez and P. K. Moore, *FASEB J.* 2005, **19**, 1196–1198.

7. K. Abe and H. Kimura, *J. Neurosci.* 1996, **16**, 1066–1071.

8. C.K. Nicholson and J.W. Calvert, *Pharmacol. Res*. 2010, **62**, 289–297.

9. (a) D. Giuliani, A. Ottani, D. Zaffe, M. Galantucci, F. Strinati, R. Lodi and S. Guarini, *Neurobiol. Learn. Mem,* 2013, **104**, 82. (b) K. Eto, T. Asada, K. Arima, T. Makifuchi and H. Kimura, *Biochem. Biophys. Res. Commun.* 2002, **293**, 1485–1488.

10**.** (a) P. Kamoun, M.C. Belardinelli, A. Chabli, K. Lallouchi and B. Chadefaux-Vekemans, *Am. J. Med. Genet.* 2003, **116A**, 310–311. (b) L. F. Hu, M. Lu, C. X. Tiong, G. S. Dawe, G. Hu and J. S. Bian, *Aging Cell,* 2010, **9**, 135.

11. W.Yang, G. Yang, X. Jia, L. Wu and R. Wang*, J. Physiol.* 2005*,* **569***,* 519–531.

12. S. Fiorucci, E. Antonelli, A. Mencarelli, S. Orlandi, B. Renga, G. Rizzo, E. Distrutti, V. Shah and A. Morelli, *Hepatology*., 2005, **42**, 539–548.

13. C. Liu and S. Shen, *Anal. Chem.*, 1964, **36**, 1652-1654.

14. (a) N. S. Lawrence, J. Davis, L. Jiang, T. G. J. Jones, S. N. Davies and R. G. Compton, *Electroanalysis* 2000, **18**, 1453–1460; (b) I. S. P. Savizi, H.-R. Kariminia, M. Ghadiri and R. Roosta-Azad, *Biosens. Bioelectron.,* 2012, **35**, 297-301.

15.(a) J. Čmelik, J. Machat, V. Otruba and V. Kanicky, *Talanta*, 2010, **80**, 1777-1781; (b) J. M. Davidson, Z. Pikramenou, A. Ponce and R. E. P. Winpenny, *Anal. Chem.*, 2009, **81**, 3669-3675.

16. A. Safavi and M. A. Karimi, *Talanta,* 2002, **57**, 491-500.

17. (a) J. Furne, A. Saeed and M. D. Levitt, *Am. J. Physiol*. 2008, **295**, R1479–R1485; (b) S. E. Mylon and G. Benoit, *Environ. Sci. Technol.*, 2001, **35**, 4544-4548; (c) J. Radfordknoery and G. A. Cutter, *Anal. Chem.*, 1993, **65**, 976-982.

18.(a) V.S. Lin, W. Chen, M. Xian and C.J. Chang *Chem. Soc. Rev.***,** 2015**, 44,** 4596—4618; (b) B. Peng and M. Xian *Asian J. Org. Chem.* 2014**, 3**, 914 – 924.

19. (a) Y. Yan, H. Yu, Y. Zhang, K. Zhang, H. Zhu, T. Yu, H. Jiang and Wang, S. *ACS Appl. Mater. Interfaces* 2015, **7**, 3547; (b) T. Liu, J. Lin, Z. Li, L. Lin, Y. Shen, H. Zhu and Y. Qian, *Analyst* 2015, **140**, 7165; (c) L. Yang, X. Liu, L. Gao, F. Qi, H. Tian and X. Song, *RSC Adv.* 2015, **5,** 98154; (d) Y. Cai, L. Li, Z. Wang, Sun, Z. J. A. Qin and B. Z. Tang, *Chem. Commun.* 2014,52, 8892; (e) L. He, W. Lin, Q. Xu and H. Wei, *Chem. Commun.* 2015, **51**, 1510; (f) X.L. Liu, X.J. Du, C.-G. Dai and Q.-H. Song, *J. Org. Chem.* 2014, **79,** 9481. (g) K. Maiti, A.K.Mahapatra, R.Maji, S.Mondal, S.S.Ali, A.Gangopadhyay, S.K.Manna and S.Mandal, *Chemistry Select*, 2016, **1**, 5066-5073.

20**.**(a) H. Li, Q. Yao, J. Fan, N. Jiang, J. Wang, J. Xia and X. Peng, Chem. *Commun*. 2015, **51**, 16225; (b) Y. Qian, J. Karpus, O. Kabil, S.-Y. Zhang, H.-L. Zhu, R. Banerjee, J. Zhao and C. He, *Nat. Commun*. 2011, **2**, 495; (c) J. Liu, Y.-Q. Sun, J. Zhang, T. Yang, J. Cao, L. Zhang and W. Guo, *Chem. Eur. J.* 2013, **19**, 4717; (d) X. Wang, J. Sun, W. Zhang, X. Ma, J. Lv and B. Tang, *Chem. Sci*. 2013, **4,** 2551; (e) Y. Chen, C. Zhu, Z. Yang, J. Chen, Y. He, Y. Jiao, W. He, L. Qiu, J. Cen and Z. Guo, *Angew. Chem., Int. Ed*. 2013, **52**, 1688.

21. (a) V. S. Lin and C. J. Chang, *Curr. Opin. Chem. Biol.,* 2012, **16**, 595-601; (b) A. R. Lippert, *J. Inorg. Biochem.*, 2014, **133**, 136-142; (c) R. Wang, F. Yu, L. Chen, H. Chen, L. Wang and W. Zhang, *Chem. Commun.*, 2012, **48**, 11757-11759.

22. Q. Li and J. R. Lancaster, *Jr., Nitric Oxide* 2013, **35**, 21 –34.

23. A. R. Lippert, E. J. New, C. J. Chang, *J. Am. Chem. Soc*. 2011, **133**, 10078.

View Article Online
DOI: 10.1039/C7NJ04632D

24. H. Peng, Y. Cheng, C. Dai, A. L. King, B. L. Predmore, D. J. Lefer and B. Wang, *Angew. Chem., Int. Ed*. 2011, **50**, 9672.
25. S. K. Das, C. S. Lim, S. Y. Yang, J. H. Han and B. R. Cho, *Chem. Commun*. 2012, **48**, 8395.

26. L. A. Montoya and M. D. Pluth, *Chem. Commun*. 2012, **48**, 4767.

27. Q. Wan, Y. Song, Z. Li, X. Gao and H. Ma, *Chem. Commun*. 2013, **49**, 502.

28. Z. Wu, Z. Li, L. Yang, J. Han and S. Han, *Chem. Commun*. 2012, **48**, 10120.

29. F. Yu, P. Li, P. Song, B. Wang, J. Zhao and K. Han, *Chem. Commun*. 2012, **48**, 2852.

30. S. Chen, Z.-j. Chen, W. Ren and H.-w.Ai*, J. Am. Chem. Soc.* 2012, **134**, 9589.

31. Y. Qian, J. Karpus, O. Kabil, S.-Y. Zhang, H.-L. Zhu, R. Banerjee, J. Zhao and C. He, *Nat. Commun*. 2011, **2**, 495.
32.(a) X. Cao, W. Lin, K. Zheng and L. He, *Chem. Commun*. 2012, **48**, 10529.

33. A. K. Das, S. Goswami , C. K. Quah and H. K. Fun, *New J. Chem.,* 2015, **39**, 5669-5675.

34. P. Qi, D. Zhang, Y. Suna and Y. Wana, *Anal. Methods*, 2016, **8**, 3339-3344.

35. L. He, X. Yang, K. Xu, X. Kong and W. Lin, *Chem. Sci*., 2017, **8**, 6257.

36. (a) S. Chen, P. Hou and X. Z. Song, *Sens. Actuators, B*, 2015, **221**, 951–955. (b) J. M. Wang, H. Yu, Q. Li and S. J. Shao, *Talanta,* 2015, **144**, 763–768. X. J. Yang, L. Q. Shen, H. B. Bao, X. X. Fang, J. W. Xu, Y. X. Zhao and W. Yang, *Sens. Actuators*, *B*, 2015, **220**, 1361–1367.

37. Q. Huang, X. F. Yang and H. Li, *Dyes Pigm*., 2013, **99**, 871–877. C. H. Zhang, B. Peng, W. Chen, S. M. Shuang, M. Xian and C. Dong, *Dyes Pigm.,* 2015, **121**, 299–304. X. Li, J. Cheng, Y. L. Gon, B. Yang and Y. Z. Hu, *Biosens. Bioelectron*., 2015, **65**, 302–306.

38. (a) H. Zhang, C. Zhang, R. Liu, L. Yi and H. Sun *Chem. Commun.,* 2015, **51**, 2029-2032; (b) H. Zhang, C. Zhang, R. Liu, L. Yi and H. Sun *Chem. Commun.***,** 2015, **51**, 2029; (c) H. Zhang, P. Wang, Y. Yang and H. Sun, *Chem. Commun*., 2012, **48**, 10672; (d) J. Jo and D. Lee, *J. Am. Chem. Soc*., 2009, **131**, 16283.

View Article Online
DOI: 10.1039/C7NJ04632D

Graphical abstract

Reaction-Based Bi-signaling Chemodosimeter Probe for Selective Detection of Hydrogen Sulfide and Cellular Studies

Uday Narayan Guria,[a] Kalipada Maiti,[a] Syed Samim Ali,[a] Sandip Kumar Samanta,[a] Debasish Mandal,[b] Ripon Sarkar,[c] Pallab Datta,[c] Asim Kumar Ghosh,[d] Ajit Kumar Mahapatra*[a]

[a] Department of Chemistry, Indian Institute of Engineering Science and Technology, Shibpur, Howrah-711103, West Bengal, India, Email: akmahapatra@rediffmail.com, Fax: +913326684564

[b] School of Chemistry and Biochemistry, Thapar Institute of Engineering and Technology, Patiala 147 004 Punjab, 486 India.

[c] Centre for Healthcare Science and Technology, Indian Institute of Engineering Science and Technology, Shibpur, India

[d] Bhabha Atomic Research Centre,Trombay.Mumbai-400085, India.